Welding in the World
https://doi.org/10.1007/s40194-025-02032-3

RESEARCH PAPER

Welding of 42SiCr treated by quenching and partitioning—mechanical properties of the HAZ and preheating proposal

Jonny Kaars[1] · Fabian Dittrich[2] · Peter Mayr[3] · Jonas Hensel[1]

Received: 9 September 2024 / Accepted: 27 March 2025

Abstract
A 42SiCr experimental steel was heat-treated by the quenching and partitioning (Q&P) heat treatment to achieve a combination of high strength and ductility. The associated microstructure is characterized in literature by finely distributed martensite laths with a small volume fraction of retained austenite embedded. The goal of this work is to provide a comprehensive characterization of the mechanical properties of all subzones in the heat-affected zone (HAZ) of welded 42SiCr-Q&P steel. Dedicated microspecimens were subjected to a specifically selected thermal cycle in a dilatometer and characterized by mechanical testing and microstructural assessment. One specimen series is dedicated to the assessment of the mechanical properties of the material after welding; another four specimen series represent some carefully selected strategies to mitigate adverse effects of welding. Tensile testing revealed a decrease in yield strength in the HAZ by up to 35%. The ductility of the material showed inverse behavior. Material in the supercritical zone shows > 2000 MPa of ultimate strength, but at the same time is very brittle. The most remarkable result showed that the embrittlement in the supercritical zone can be successfully mitigated by holding the material at temperatures in the range of 200–250 °C for 5 min upon cooling, resulting in a yield strength of around 1400 MPa along with a ductility of > 10%, restoring the desired property combination. This very promising observation suggests fusion welding of 42SiCr-Q&P might be possible by means of preheating, maintaining the superior mechanical properties of Q&P in the weld.

Keywords Quenching and partitioning · 42SiCr · HAZ · Welding · Tensile strength · Fracture strain · Hardness

1 Introduction

Since the first description of the quenching and partitioning (Q&P) treatment by [1, 2], this material concept has evolved into commercially available 3rd generation advanced high strength steels [3], being first commercialized as QP980 by Baosteel in 2012 [4]. The goal of the Q&P heat treatment is to achieve a microstructure consisting of finely dispersed martensite laths with embedded retained austenite in between [5]. While the martensite contributes to the remarkable strength of the material, the embedded austenite provides improved ductility during plastic deformation [6, 7]. De Moor et al. [8] reported that the austenitic phase exhibits the TRIP effect during deformation; this was later confirmed by [9]. [10] measured a significant volume fraction of retained austenite in Q&P steel, but still stated that its distribution cannot be determined by light microscopy or electron beam microscopy as it is presumed as very thin foil-like particles. Ariza-Echeverri et al. [9] later confirmed this assumption.

While commercial Q&P steels are available with yield strengths of about 1000 MPa [4, 11] along with about 13% strain to fracture, laboratory data suggests that the true potential of this material group has not been industrialized yet. The experimental steel 42SiCr first introduced by Masek et al. [12] with different Q&P routines applied to it provided

Recommended for publication by Commission IX - Behaviour of Metals Subjected to Welding.

Jonny Kaars
jonny.kaars@mb.tu-chemnitz.de

Fabian Dittrich
fabian.dittrich@b-tu.de

Peter Mayr
peter.mayr@tum.de

Jonas Hensel
jonas.hensel@mb.tu-chemnitz.de

1 Chemnitz University of Technology, Chemnitz, Germany

2 Brandenburg University of Technology Cottbus-Senftenberg, Cottbus, Germany

3 Technical University of Munich, Garching, Germany

Published online: 10 April 2025

excellent results. Data provided by Jirkova et al. [10] on 42SiCr shows that up to 2000 MPa tensile strength are possible, while simultaneously providing up to 20% strain to fracture. Especially the combination of strength and ductility is yet unmatched by existing steel grades and provides far superior energy absorption during deformation as well as robustness against local overloading by means of local plasticity. Figure 1 depicts the potential of 42SiCr in comparison to existing automotive steels. Cerny et al. [13] also reported an excellent fatigue strength of 42SiCr with Q&P treatment. Q&P thermal parameters yielding more retained austenite provide better fatigue performance [14]. The Q&P routine can be readily implemented in existing press-hardening lines [15, 16], or integrated into forming lines [17].

Somani et al. [18] mentioned the formation of bainite in Q&P steels and pointed out that the final fraction of retained austenite varies in a complex manner depending on thermal profiles and metallurgical prerequisites. By means of dilatometric experiments, Jenicek et al. [19] measured significant bainitic transformation during the partitioning phase. The more pronounced the bainite formation was, the higher the partitioning temperature was. The chromium content of 42SiCr is necessary to obtain ferrite-free martensite, as reported by Jirkova et al. [20]. The yield strength of 42SiCr is decreased, as the prior austenite grain size increases [21], although within certain limits, the mechanical properties of 42SiCr can be tailored by selection of the thermal parameters in the Q&P process [22]. Recent developments employ machine learning models on the prediction of Q&P properties [23]. A commercial steel AISI4340 recently was successfully Q&P heat-treated to obtain a yield point of about 1500 MPa along with 12% elongation to fracture [24].

One challenge that always must be met by new steel grades is a sufficient weldability under industrial conditions. While comprehensive data on fusion welding of commercial Q&P grades exists, only few works elaborate on welding results on more advanced laboratory Q&P grades.

Wang et al. [25] reported increased hardness due to the formation of martensite in the HAZ of spot-welded Q&P steel. Spena et al. [26] later attributed interfacial failure mode of spot-welded Q&P to this martensite. The first more detailed work on laser welding of 42SiCr with Q&P was presented by Pekovic et al. [27]. A maximal hardness up to 700 HV1 in the molten zone as well as softening to about 400 HV1 in the HAZ was reported. Nadimi et al. [28] determined that the softening effect in the HAZ below A_{c1} is inversely proportional to the prior martensite volume fraction in the base metal. In spot welding of commercial QP980, the failure mode was successfully improved by [29, 30] by means of the reheating effect of a second current pulse. Process parameter windows to spot-weld commercial Q&P steel are similar to existing dual-phase steel [31]. Induction welding of pipes made of 42SiCr is reported by Kroll et al. [32] wherein the Q&P treatment was performed after the welding process. The Q&P properties could be fully restored in the welded region of the pipes. Previous work [33] showed that the dilatometer is capable of accurately representing the thermal cycles of actual welding processes. Later, Xue et al. [34] employed a gleeble apparatus to produce samples of individual HAZ subzones on laser-welded commercial QP980.

Summarized, a major research gap, which is addressed by this work, exists in literature: There is no data available on yield and ultimate strength and strain to fracture in the relevant subzones of the heat-affected zone (HAZ) of fusion welds performed on Q&P-treated 42SiCr steel. Previous work only elaborated on hardness in the HAZ [33]. Furthermore, no attempts have been made to mitigate adverse microstructural conversions at welds on the material. This work includes a first insight into the results of welding heat management strategies on this Q&P steel, such as annealing, preheating, and preheating along with post-weld reheating in context to the fusion welding thermal cycle. Data on the mechanical performance of the material after

Fig. 1 Potential of QP steel (yellow) in the Global Formability Diagram, based on [3]

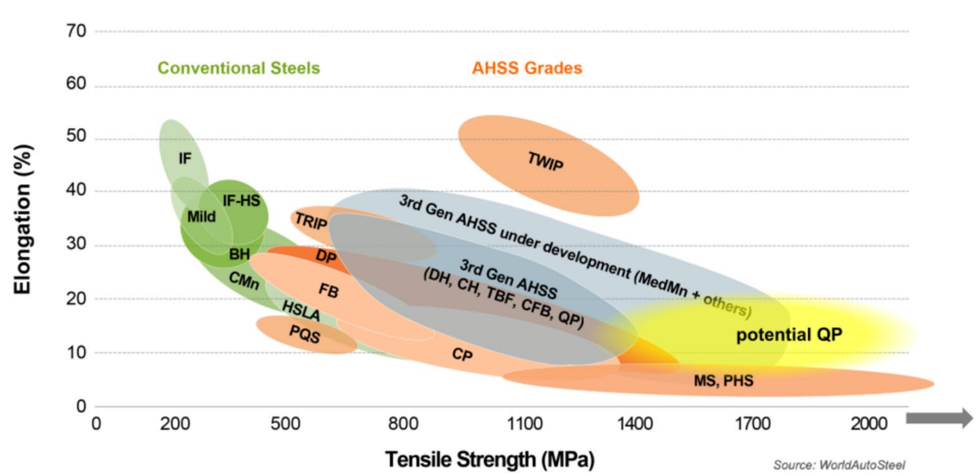

Table 1 Composition and carbon equivalent of 42SiCr steel used in this work

Element	C	Si	Cr	Mn	Fe	CEV
wt%	0.42	2.0	1.3	0.68	bal.	0.82

Table 2 Martensitic conversion temperatures of 42SiCr [20]

	Ms	Mf
°C	298	178

those treatments is being presented as well. As 42SiCr is not commercially available yet, raw material is scarce and filler materials not available at all. Therefore, all the experiments of this work have been carried out in a thermo-mechanical simulation apparatus, a dilatometer.

2 Materials and methods

2.1 Material preparation and characterization

The material 42SiCr was delivered as hot-rolled sheet metal strips. Only a small batch of raw material was available, as it is not commercially produced yet, which resulted in the size of the specimens used in this work being as small as possible, and specimen numbers to be very carefully selected for each experiment. The chemical composition along with the calculated carbon equivalent according to IIW - CEV - is listed in Table 1 [20] determined martensitic conversion in 42SiCr to start at 298 °C, cf. Table 2.

Figure 6(a) shows an optical micrograph of the perlitic-ferritic microstructure of 42SiCr in as-delivered state, with the white areas being the ferrite and the darker areas being the perlite. Thermodynamic equilibrium calculations using the software MatCalc version 5.62 (rel 1.006) and the database mc_fe_2.059.tdb confirm the observed perlitic-ferritic microstructure in the as received sheet material. Sheet metal specimens for tensile testing were fabricated as follows: Raw material of 1.5 mm thickness was heat-treated using the QP routine described in the "Thermal cycle" section by using a heated press for quenching and a lab oven for partitioning. The sheets were cut to smaller rectangular strips by a water jet, whose midsection was then heat-treated to the specific thermal cycle in the dilatometer. After dilatometer heat treatment, the specimens were machined to the final tailored contour using wire erosion and fine-ground from both sides to the final thickness of 0.9 mm. The grinding was also employed to remove a decarburized layer from the specimens, cf. [33] for details. In order to be able to perform tensile tests, additional clamping tabs of mild steel were laser-welded to the small QP specimens using nickel-based filler material. Figure 2 depicts a prepared specimen and its major dimensions right before the tensile test. The specimen geometry was selected based on a suggestion made by Prof. Bohuslav Masek, the author of [12].

Additional, cylindrical specimens of 5 mm diameter and 10 mm length were milled from a single material piece of 10 mm thickness. These specimens underwent most of the investigated thermal cycles in the dilatometer. They were used to measure the dilatation of the material due to microstructural conversions, and obtain light microscopic images on microsections, both of which could not be obtained on the tensile samples. Tensile tests according to ISO 6892 - 1 were performed on a Zwick-Roell universal testing machine, while the strain of the specimen was monitored with a video-extensiometer using a GOM Aramis camera system. To enable the optical strain measurement, each specimen was coated with a special contrasting spray right before the tensile test began. Out of the tested pool, the more ductile specimen ruptured in the parallel testing length, the less ductile specimen tended to rupture at the ends of the parallel length. Due to the optical strain measurement, valid strain data was obtained in both cases. Microstructural investigations were carried out after employing standard metallographic practices (grinding, polishing, and etching). For light-optical microscopy, a Zeiss Axiovert 200 MAT microscope was used, while hardness measurements were conducted using a Struers DuraScan 70.

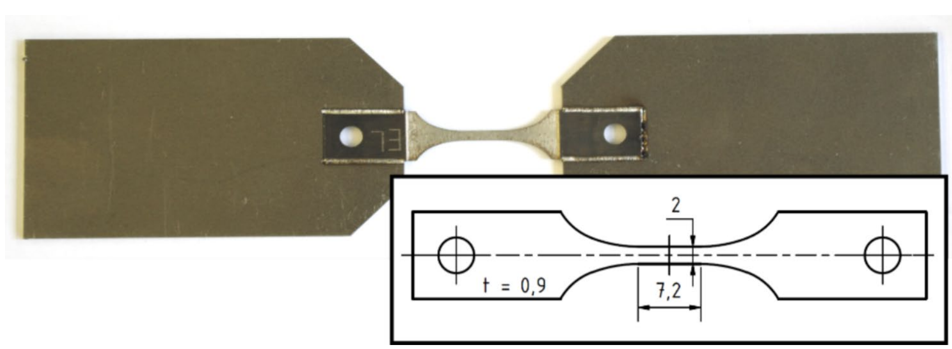

Fig. 2 42SiCr sheet metal specimen and its major dimensions, specimen prepared for tensile testing with laser-welded clamp tabs

2.2 Thermal cycle

All specimens in this work were subject to two thermal cycles: quenching and partitioning followed by a cycle to generate the heat-affected zone, which would have resulted from welding. Both cycles were applied to the specimens using a Baehr dilatometer DIL805 A/D. Q&P was immediately followed by the welding thermal cycle without removing the individual specimen from the dilatometer. Raw material after Q&P treatment in the following is noted as 42SiCr+QP. Welding thermal cycles following the Q&P cycle had two main goals, the first goal being the characterization of strength and ductility of the HAZ. The second goal was to explore possible thermal cycle modifications to mitigate formation of microstructures being overly brittle or overly softened. The temperature profiles below represent measured data.

2.2.1 Quenching and partitioning

The Q&P heat treatment consisted of heating up of the sample to 950 °C and holding for 150 s followed by quenching the sample to 200 °C with a cooling rate of 40 K/s. The sample was then partitioned at 250 °C for 300 s before it was cooled down to room temperature, cf. Fig. 3 (a). The schedule is oriented on schedule 2 published in [15] and was used in [33] before.

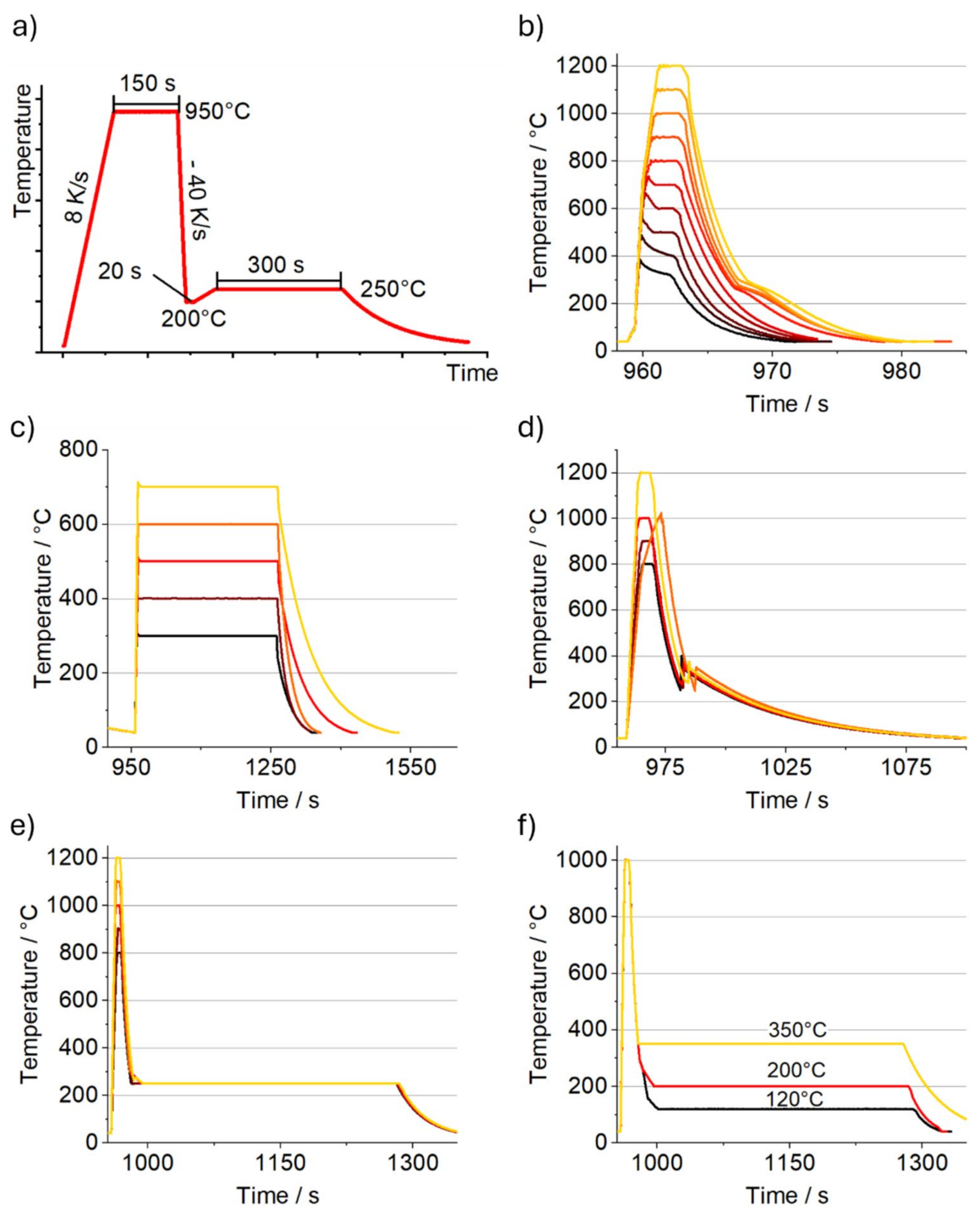

Fig. 3 Thermal cycles used: **a** quenching and partitioning; **b** HAZ thermal cycles, measured data; **c** annealing of 42SiCr+QP, 300 s dwell time depicted; **d** brief reheating from 250 to 350 °C during cooling after welding; **e** welding thermal cycle, cooling after welding interrupted at 250 °C for 300 s; **f** welding thermal cycle, cooling after welding interrupted for 300 s at various temperatures

2.2.2 Heat-affected zone

HAZ simulation was performed for peak temperatures from 300 to 1200 °C in steps of 100 °C, with 3 specimens per temperature, cf. Fig. 3 (b). Heating to peak temperature was performed with 1 kK/s; then, the temperature was held for 4 s, followed by cooling according to Newton's cooling law. The cooling speed was set based on the time between 800 and 500 °C (t8/5) as shown in Table 3.

For specimens not reaching 800 °C, the cooling curve was computed according to Newton's law considering a fictive t8/5. Specimens below 800 °C peak temperature showed some overshooting in the heating phase, while specimens with peak temperature of 800 °C or more show a distinguished kink in the cooling curve resulting from martensitic conversion. Both deviations are attributed to imperfections of the apparatus' temperature controller mechanism. In a previous work [33], it was shown that neither dwell time nor heating/cooling rates have significant effects on HAZ properties of 42SiCr+QP. Consequently, in this work, only one representative welding cycle with heating rates and dwell times as described was simulated. The approach conformed well with the scarcity of the raw material.

2.2.3 Annealing

An annealing thermal cycle was applied in order to investigate the susceptibility of the material in the Q&P state to softening due to heating. Only temperatures below A_{c1}, namely from 300 to 700 °C in steps of 100 °C, were investigated in order to avoid diffusionless lattice transformations. The heat-up was done with 1 kK/s; the dwell time at annealing temperature was varied in two stages, 150 s and 300 s. Figure 3 (c) shows measured data of the thermal cycle.

The goal of the annealing cycle was to determine which effect pre- or post-heating of 42SiCr in conjunction with welding may have on the material properties. This information is also relevant in order to estimate the effect of low temperature dwell times in the HAZ being much longer than previously investigated.

2.2.4 Reheating pulse

Other than the annealing thermal cycle, this cycle focuses on the portions of the HAZ surpassing A_{c1}, thus at least partially transforming from the austenitic phase upon cooling. The reheating pulse is characterized by a HAZ cycle as described before, whose cooling branch is interrupted at 250 °C by a very brief reheating to 350 °C, and then continuing the cooling process, cf. Fig. 3 (d). The superordinated goal of the pulse cycle was to avoid formation of brittle, purely martensitic microstructures in the transformed areas of the HAZ. The pulse had fusion welding processes such as laser and resistance spot welding in mind, where a very brief reheating is technically easy to implement. The pulse aimed at mimicing the Q&P cycle a bit by interrupting the formation of martensite during cooling.

Table 3 Cooling rate parameters for HAZ

Peak temperature/°C	$t_{8/5}$ / s
300 – 600	12
700	8
800 – 1000	4.5
1100 – 1200	4

2.2.5 Interrupted cooling at 250 °C after welding

This cycle focuses on the portions of the HAZ surpassing A_{c1} and countering their brittleness as well. After completing the HAZ cycle as described before, the cooling branch once again is interrupted at 250 °C, this time holding 250 °C for 300 s, cf. Fig. 3 (e) for a depiction of measured data. The approach was colloquially named "Catch 'n Hold" by the authors and will be denoted this way in the following. The idea of this cycle was simple: interrupt cooling roughly in the middle between martensite start and finish temperature, cf. Table 2, and then hold the temperature long enough to allow for diffusion-driven effects, i.e., the stabilization of retained austenite by carbon diffusion. From the technological point of view, this cycle would be easy to implement by means of preheating before fusion welding.

2.2.6 Interrupted cooling at various temperatures after welding

This cycle is related to the Catch 'n Hold cycle previously described, the only difference being the temperature at which the cooling phase is interrupted, cf. Fig. 3 (f). Again, the goal was to counter brittle martensitic microstructures in the HAZ. The experiments were aimed to give insight into three strategies: interruption of cooling at 350 °C, just before martensitic transformation to commence and investigate the resulting microstructure. Second, putting the dwell temperature of 200 °C closer to martensite finish temperature to vary the martensite content compared to the previous experiment. Third, interrupt cooling at 120 °C, right below martensite finish temperature, and investigate the resulting microstructure.

3 Results and discussion

Based on the dilatation curves measured in this work, the transition temperatures were determined to be at 790 °C and 826 °C respectively, while the martensitic conversion

Table 4 Conversion temperatures of 42SiCr, measured

	A_{c1}	A_{c3}
°C	790	826

Table 5 Mechanical properties of 42SiCr+QP used in this work

	H/HV1	$R_{p0,2}$/MPa	R_m/MPa	A_g/%	A/%
Value	579	1290	1938	4,7	10,4
SD	10.2	102	21	0.26	0.75

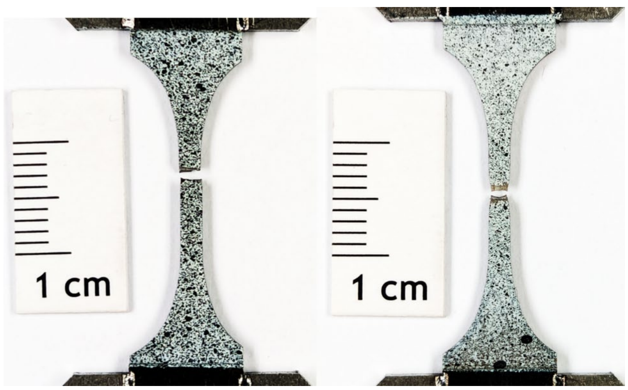

Fig. 4 Specimen after tensile testing; left, HAZ 1100 °C peak temperature; right, Catch and Hold at 350 °C for 300 s; specimen width was reduced by 31.7% due to necking on the sample shown

temperatures given by Jirkova et al. [20] were confirmed, cf. Table 4.

The microstructure of 42SiCr+Qp, as depicted in Fig. 6 (b), shows a very fine-grained martensitic matrix, presumably with finely distributed retained austenite. The latter was not detectable with the investigation methods used in this work, but was measured by Mehner et al. [35] on the same alloy. Tensile testing of 42SiCr+QP determined the ultimate tensile strength to be 1938 MPa along with an elongation at fracture of 10.4%. Hardness and yield strength were more moderate, amounting to 579 HV1 and 1290 MPa, respectively, cf. Table 5. The distinct hardening during plastic deformation suggests deformation induced martensitic transformation of retained austenite.

The combination of strength and ductility of 42SiCr is outstanding. The work absorbed during deformation can be roughly characterized by the product of ultimate tensile strength and elongation at rupture, i.e., a measure for the surface area under the stress-strain curve. Compared to the widely used press-hardening steel 22MnB5, 42SiCr+QP has 30% more ultimate tensile strength, but absorbs about double the amount of energy during deformation. Figure 4 gives an exemplary insight into the fracture behavior of the samples tested. The left one fractured very brittle without noticeable necking, while the right one exhibits significant necking.

3.1 HAZ properties

Mechanical properties of the HAZ of welded 42SiCr+QP are presented in Fig. 5. Starting from the base material properties, the material softens with increasing peak temperature up to a minimal yield strength of 847 MPa at 800 °C. Uniform elongation and elongation to fracture increase slightly to 6.8% and 13.4% respectively at 500 °C peak temperature, to decline again a few percent up to 700 °C. At 800 °C peak temperature, A is only very slightly larger than Ag, indicating loss of the ability to exhibit deformation hardening. Further increasing peak temperatures, i.e., peak temperatures above A_{c3}, results in increased yield strength of about 1700 MPa along with a very brittle fracture behavior characterized

Fig. 5 Mechanical properties in the HAZ of welded 42SiCr+QP

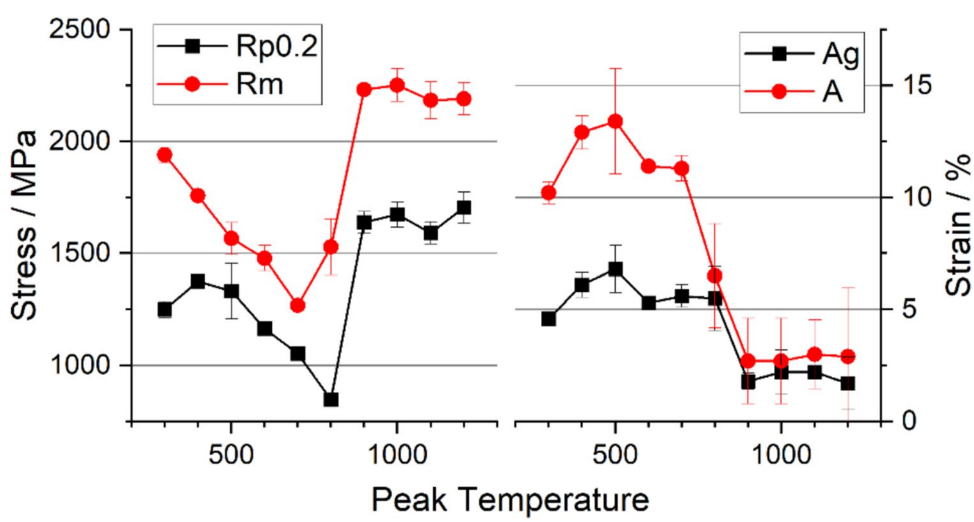

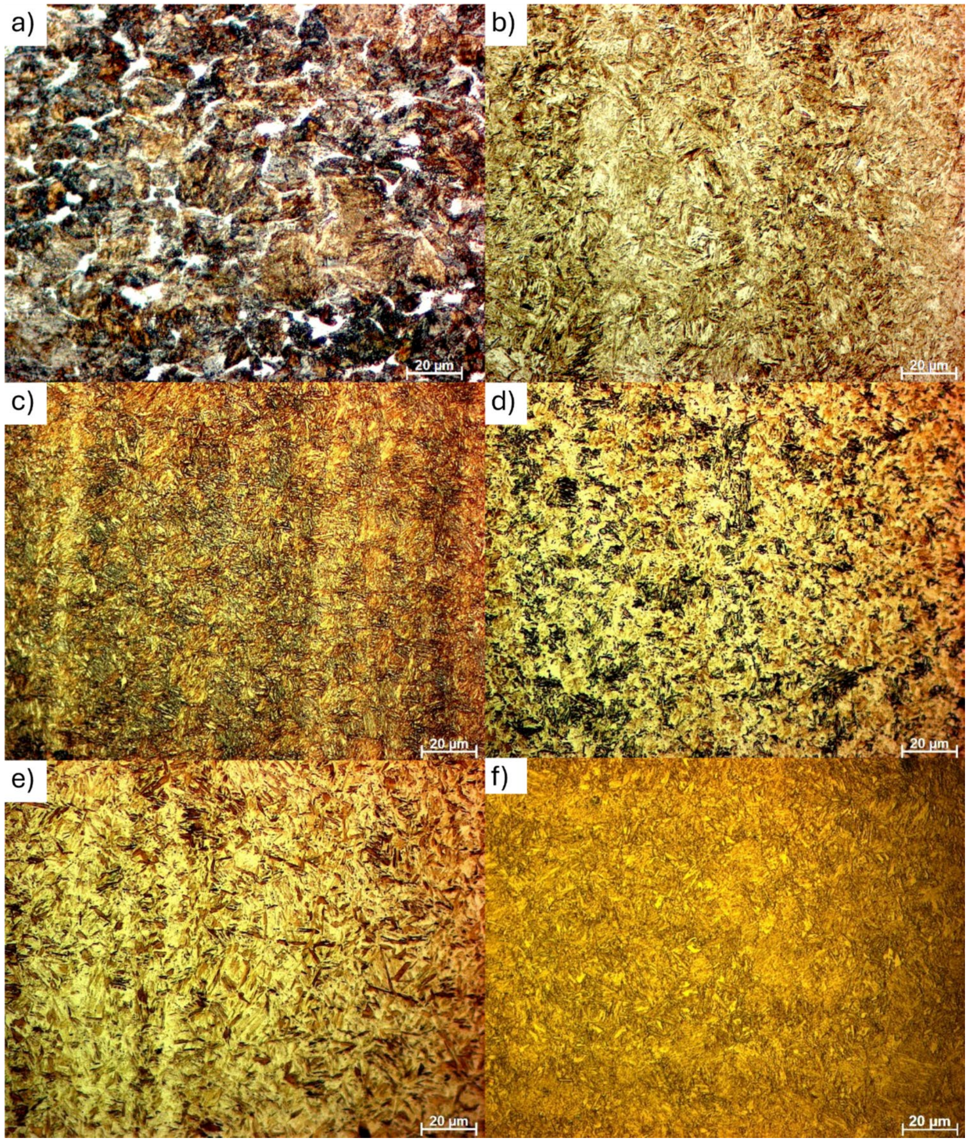

Fig. 6 **a** Microstructure of the as received 42 CrSi steel. Etched with 2%-Nital; microstructure of 42SiCr+QP after the 1000 °C cycle. **b** Microstructure of 42SiCr+QP. **c** Microstructure of 42SiCr+QP after the 500 °C cycle. **d** Microstructure of 42SiCr+QP after the 800 °C cycle; darker areas, preserved Q&P; brighter areas, freshly formed martensite. **e** Microstructure of 42SiCr+QP after the 1000 °C cycle. **f** Microstructure of 42SiCr+QP annealed at 700 °C for 300 s

by about 3% elongation to fracture. A hardness of about 700 HV1 was measured in this zone.

Microstructural images were made to better interpret the data recorded. From 300 to 700 °C peak temperature, the Q&P microstructure is still present, as shown for 500 °C in Fig. 6 (c). This changes abruptly at 800 °C, cf. Fig. 6 (d). In the darker colored parts of the sample, the original Q&P microstructure was still visible, while the brighter colored areas indicate freshly formed martensite. As 800 °C is in the intercritical zone between A_{c1} and A_{c3}, slight differences in peak temperature will result in significant changes in the volume of the microstructure that actually transforms. In turn, a mixed microstructure composed of Q&P and martensite, with a composition depending strongly on the exact peak temperature, is formed. This rationalizes the increased standard deviation in ultimate tensile strength, uniform elongation, and elongation to fracture measured at the 800 °C samples. Specimens heated above 800 °C can be characterized to consist of inhomogeneous martensite as expected, cf. Fig. 6 (e). The grain size of the prior austenite grains increases with increasing peak temperature, as microsections showed.

3.2 Heat treatment of the HAZ

3.2.1 The effect of annealing

With increasing annealing temperature, the tensile strength of 42SiCr+QP decreases, up to a minimum yield point of 924 MPa after 700 °C annealing, along with a maximum elongation to fracture of almost 15%. Figure 7 depicts the data. The softening effect is more pronounced at temperatures above 500 °C; up to that point, the annealing effect lowers the ultimate tensile strength by only 20%, while

Fig. 7 Mechanical properties of annealed 42SiCr+QP

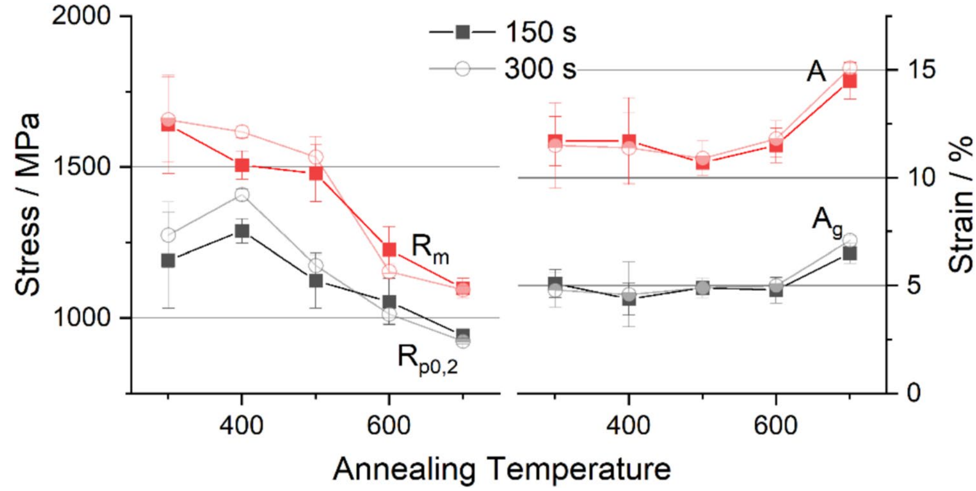

leaving the elongation nearly unaffected. Softening of the Q&P microstructure is attributed to tempering of the martensitic portion of the Q&P structure. The longer dwell times of the annealing cycle stabilize the measured properties contrary to the HAZ cycle, especially at higher temperatures. Light microscopy of the annealed specimens showed the original Q&P microstructure preserved, as shown in Fig. 6 (f) on the 700 °C specimen.

3.2.2 Effect of pulse reheating during cooling

Figure 8 shows the mechanical properties of 42SiCr+QP, whose cooling after welding was interrupted by a reheating pulse, in comparison to the original HAZ properties presented in the "HAZ properties" section. While the pulse has a negligible effect at 800 °C, it lowers tensile strength and increases elongation of the HAZ significantly at and above 900 °C. The original Q&P properties are almost restored. It has to be noted that at 1000 °C peak, only two, and at 1200 °C only one specimen was tested; the increased standard deviation of the elongation at 1000 °C is attributed to this fact. We seem to see martensite in the light microscopic microsection in Fig. 11 (a), but the tensile strength values and elongation at fracture stand in a stark contrast to this observation. It is not yet clear how the reheating impulse influences the dynamics of microstructure evolution.

3.2.3 Effect of interrupted cooling after welding

Analog to the previous section, mechanical properties of 42SiCr+QP with interrupted cooling at 250 °C according to the Catch 'n Hold thermal cycle are presented in Fig. 9. Similar to the reheating pulse, at 800 °C, the effect is negligible. At 900 °C and above, Catch 'n Hold lowers the yield point to about 1300 MPa and increases the uniform elongation to about 4.5%, greatly improving the properties of the HAZ. The standard deviation of the results tends to be smaller than

Fig. 8 Mechanical properties in the HAZ of welded 42SiCr+QP with brief reheating from 250 to 350 °C during cooling after welding

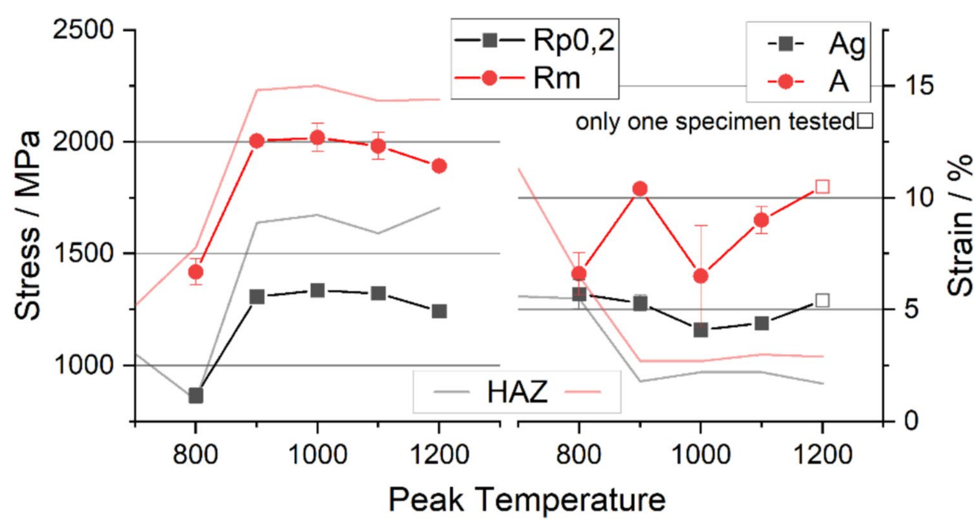

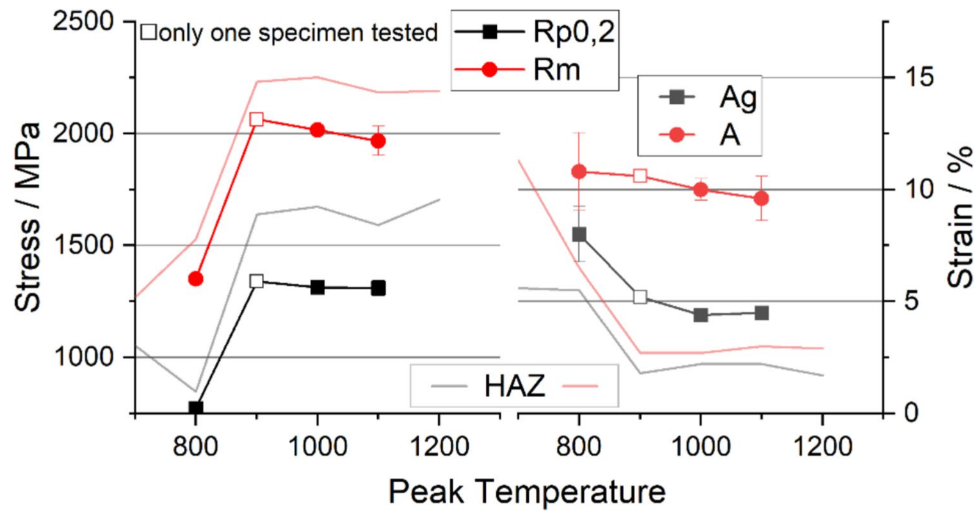

Fig. 9 Mechanical properties in the HAZ of welded 42SiCr+QP, cooling after welding interrupted for 300 s at 250 °C

that of the pulse reheat approach, but this would need to be assured by a larger number of specimens.

The microstructure of the samples produced with Catch 'n Hold is disputed, as it shows features of both the Q&P-microstructure and martensite as well. This is shown in Fig. 11(b) for a 1000 °C peak sample, and in Fig. 11(c) for one with 1200 °C peak temperature. The composition of the samples could not be determined for sure with the investigations performed, but a composition of martensite and retained austenite and/or bainite is probable. In Fig. 11(c), the enlarged prior austenite grains compared to the 1000 °C sample due to the increased peak temperature are visible. This seems to correspond to the slightly lowered tensile strength and ductility at higher peak temperatures.

Further experiments gave more insight into the role of the catch temperature; the result is displayed in Fig. 10 in comparison to the 42SiCr+QP base material and the brittle HAZ. With increasing catch temperature, the yield point is lowered from 1584 MPa at 120 °C to 1131 MPa at 350 °C respectively while the uniform elongation significantly increases from 1.5 to 5.7%. Although the relative difference between 120 and 200 °C in terms of elongation is the largest, the respective tensile strengths differ only slightly.

So far, the data shows that the mechanical properties of 42SiCr+QP can be almost restored, when cooling after welding from above A_{c3} is interrupted between 200 and 350 °C and the catching temperature is then held for 300 s. Higher catching temperatures result in softer, more ductile microstructures.

Light microscopic images of the microstructures further enhance the evaluation, cf. Fig. 11(d) to (f). The sample caught at 120 °C shows typical martensitic laths similar to those in Fig. 6 (e) although the etching is different. This observation is also supported by the mechanical performance. The 350 °C sample in Fig. 11(f) shows a very different microstructure whose composition is not yet ascertained. From a thermodynamic point of view, a mixture of bainite, martensite, and retained austenite is probable, but this could

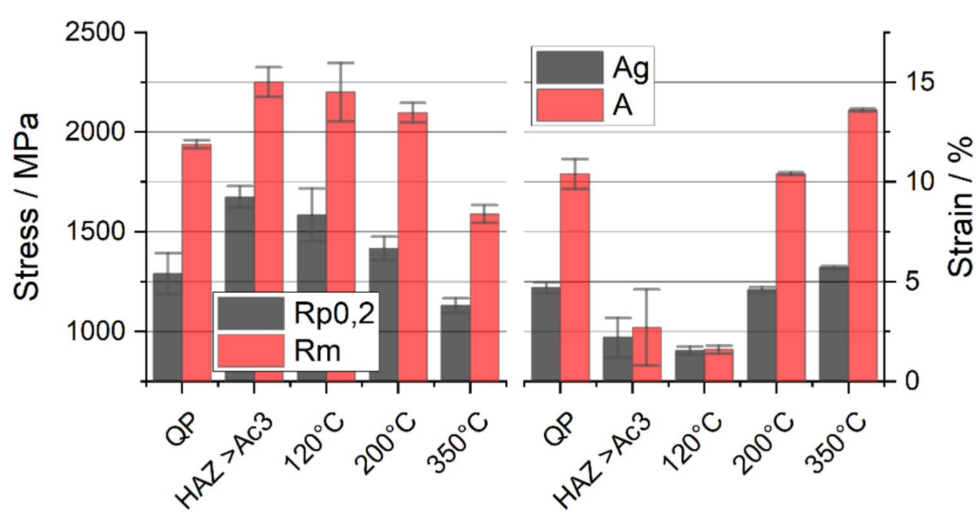

Fig. 10 Mechanical properties in the HAZ of welded 42SiCr+QP, cooling after welding interrupted for 300 s at various temperatures

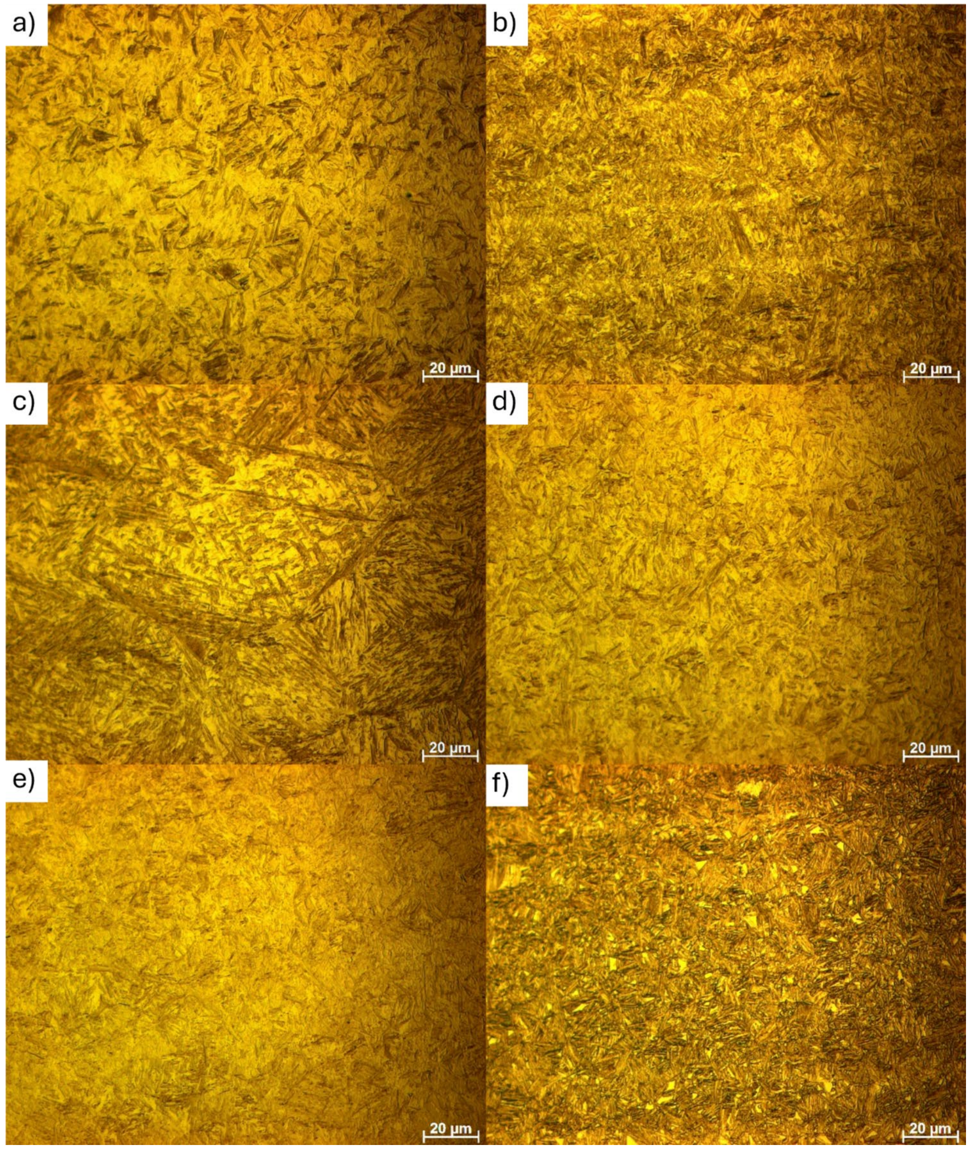

Fig. 11 Microstructure of 42SiCr+QP after **a** 1000 °C HAZ cycle followed by brief reheating to 350 °C, **b** 1000 °C HAZ cycle followed by holding at 250 °C for 300 s; **c** 1200 °C HAZ cycle followed by holding at 250 °C for 300 s; **d** 1000 °C HAZ cycle followed by holding at 120 °C for 300 s; **e** 1000 °C HAZ cycle followed by holding at 200 °C for 300 s; **f** 1000 °C HAZ cycle followed by holding at 350 °C for 300 s

not be assured via light optical microscopy. On the 200 °C sample in Fig. 11(e), a microstructure with features of both the 120 °C and the 350 °C sample is visible. The major area of the microsection seems to be martensitic, while some areas show more fine-grained features as in the 350 °C or the Q&P base material sample. Martensite predominates.

4 Summary and discussion

It became clear that much of the microstructural evolution dynamics in the welding of Q&P steel is not yet understood. Further work is required to specifically identify the portions of martensite, bainite, and retained austenite and other possibly not yet detected microstructures in the HAZ. Conveniently, a compilation of the mechanical properties in the HAZ is presented in Table 6.

Overall, the Cath 'n Hold cycle may be readily applicable in an industrial scale, as the only thing being needed to do would be preheating of the material prior to welding, and assuring it will not cool down too much during welding. The required preheating temperatures are low enough to be applicable with cheap ovens and do not require scaling protection. Obviously, the real cooling rate that will be achieved, and the resulting effect on microstructure on a preheated material needs to be investigated in the future. The subcritical zone obviously experiences changes due to tempering caused by heat in the base material, occurring at temperatures below the A_{c1} line. In [36], Gurol et al. [37] reported that decrease in the hardness in this region could be attributed to the wider grains caused by the heat cycle, although this could not be confirmed by our work.

Most importantly, coming works also must include a detailed investigation of the intercritical zone, because

Table 6 Mechanical properties in the HAZ of welded 42SiCr+QP

	Yield strength/MPa	UTS/MPa	Strain to fracture/%	Hardness/HV1
Base material	1290 ± 102	1938 ± 21	10.4 ± 0.8	579 ± 10
Subcritical zone	1050 ± 17	1268 ± 17	11.3 ± 0.6	365 ± 20
Intercritical zone	850 ± 15	1528 ± 125	6.5 ± 2.3	453 ± 73
Supercritical zone				
• Welding w/o measures	1670 ± 55	2252 ± 73	2.7 ± 1.9	700 ± 47
• Interrupted cooling, 200 °C	1416 ± 58	2097 ± 49	10.4 ± 0.1	646 ± 12
• Brief reheating 350 °C	1244	1892	10.5	652

currently in this zone the usability of the weld is limited the most. Earlier works reported hardness values similar to this work in the hardness dip of the intercritical zone before [27, 33, 38, 39], but data on strength and strain to fracture was lacking. Data from this work shows that also the ductility in the intercritcal zone is reduced along with the hardness. Kroll et al. [32] avoided the hardness dip by heat treating welded pipes only after welding.

Another focal point should be the development of suitable filler materials for 42SiCr. Furthermore, the development of the composition of 42SiCr may not be concluded, and further variants of material and thermal treatment should be investigated. Further work on the materials' fatigue strength [13] as well as the behavior when subjected to impact loading should be performed. As the retained austenite provides a finely dispersed deformation reserve, those types of loading may be particularly interesting.

Further works on specific welding processes on 42SiCr should commence, as they imply different applicability of thermal management. While in resistance spot welding, the brief reheating by a second current pulse probably may be favorable; this may not hold true for arc welding processes such as GMAW, SMAW, and TIG. Thick-walled structures like steel constructions, apparatuses, mobile cranes, and armor probably will be best welded by applying a preheating. Laser and electron beam welds on the other hand might make use of both approaches, perhaps in combination. One has to keep in mind that the material in our experiments did not melt, whereas a fusion weld will exhibit dendritic microstructures and segregations in the weld metal. Therefore, investigation of real-world welding processes will also show if the promising results presented here will hold true.

5 Conclusions

It was the goal of this work to gather insight into the characteristics of the heat-affected zone on welded 42SiCr+QP and work out chances and specify gaps of knowledge for future works. In summary, it was determined that 42SiCr, although having a relatively large carbon equivalent of 0.82, can be welded as long as the materials' characteristics are accounted for in the thermal cycle of the welding process. In low temperature areas of the HAZ up to the intercritical zone between A_{c1} and A_{c3}, notable softening of the Q&P microstructure has to be expected. This is accompanied by significant hardening and brittle fracture in areas reaching the supercritical zone above A_{c3}. The hardening effect can be effectively limited by preheating before welding or a short reheating pulse during the cooling phase. Thermal measures did not improve properties in the intercritical zone, which remains the most impaired zone after welding. The following results were obtained:

- Lower temperature, sub-critical areas of the HAZ below A_{c1} soften during welding due to the tempering of martensite. 42SiCr+QP softens with increasing peak temperature up to a minimal yield strength of 1053 ± 17 MPa at 700 °C. Compared to the base material, the yield strength is reduced by 18.4%. Uniform elongation and elongation to fracture increase slightly to 6.8% and 13.4% respectively at 500 °C peak temperature, to decline a again a few percent up to 700 °C. Any point in the annealed subcritical zone has a higher ductility and lower yield strength than the base material. The lowest hardness was measured at 700 °C, amounting to 365 ± 19 HV1.
- In the intercritical zone, the lowest yield strength of the whole HAZ of 847 ± 15 MPa with a hardness of 453 ± 73 HV1 was measured. Compared to the base material, the yield strength is lowered by 35%. While the uniform elongation of 5.5% in the zone stays on the level of the base material, the elongation at fracture is reduced by about 40 to 6.5%. Microsections revealed that the changes in mechanical behavior are attributed to partial transformation of the Q&P microstructure to martensite. Depending on the actual peak temperature reached in a location, the volume fraction of freshly formed martensite varies, resulting in varying mechanical properties in this zone. Based on the data in this work, the mechanical characteristics of the intercritical zone do not respond to pre- or post-heating.
- Significant hardening up to a yield point of 1700 MPa along with about 3% elongation to fracture occurs in the supercritical HAZ heated above A_{c3}. The average

hardness amounts to 699 ± 31 HV1. Hardening of the material is attributed to formation of martensite during the cooling phase after welding.

- Annealing of 42SiCr+QP for up to 5 min has little effect, as long as it occurs at or below 500 °C. Annealing at 700 °C lowers the yield point by 29%. Up to 600 °C uniform elongation and elongation at fracture remain nearly unchanged, while at 700 °C both increase to 7.1% and 15.1%, respectively. Consequently, pre- or post-heating of 42SiCr with up to 500 °C is feasible.
- Significant improvements of the mechanical properties in the supercritical HAZ can be achieved by interrupting the cooling phase at temperatures around the martensite start temperature and then holding the temperature for 5 min. At 200 °C dwell temperature, a yield point 10% higher than the base material along with the same elongation to fracture as the base material results from this strategy. At 250 °C dwell temperature, the base material properties are restored, while at 350 °C, the yield strength is lowered compared to the base material. Microstructural investigations could not ascertain whether these improvements may be attributed to restoration of the Q&P structure or are a result of the formation of bainite, retained austenite, or both. Nonetheless do these results suggest that the formation of brittle structures in the supercritical HAZ be avoided by preheating of the metal. The resulting properties can be tailored by choice of the preheating temperature.
- A very brief reheating from 250 to 350 °C during the cooling phase after welding yields similar strength and elongation as interrupted cooling at 250 °C. Nevertheless, the observed microstructures differ from those achieved by interrupted cooling, and could not be clearly attributed to martensite, bainite, or retained austenite in this work. The "brief reheating strategy" is very interesting because it may be very practical.

42SiCr+QP will have a substantial impact in the field of advanced high strength steel, as it provides excellent mechanical properties throughout the HAZ when treated accordingly. Additionally, its alloying concept allows cheap production at the same cost as a mild steel, but the mechanical performance is outstanding, even in comparison to other high strength steels.

Acknowledgements The authors would like to thank Prof. Bohuslav Mašek for pointing us on the topic and providing the investigated raw material.

Author contribution Conceptualization: Kaars, Dittrich. Data curation: Kaars, Dittrich. Formal analysis: Kaars, Dittrich. Funding acquisition: n.a. Investigation: Kaars, Dittrich. Methodology: Kaars, Dittrich. Project administration: Kaars, Hensel, Mayr. Software: n.a. Resources: Hensel, Mayr. Supervision: Hensel, Mayr. Validation: Kaars, Dittrich, Hensel, Mayr. Visualization: Kaars, Dittrich. Writing—original draft: Kaars. Writing—review and editing: Dittrich, Hensel, Mayr

Funding Open Access funding enabled and organized by Projekt DEAL. All work was funded internally by Chemnitz University of Technology.

Data availability The data that support the findings of this study is available from the corresponding author upon reasonable request.

Declarations

Competing interests The authors declare no competing interests.

References

1. Speer JG, Assunção FCR, Matlock DK, Edmonds DV (2005) The "quenching and partitioning" process: background and recent progress. Mater Res 8:417–423. https://doi.org/10.1590/S1516-14392005000400010
2. Streicher AM, Speer JG, Matlock DK, Coman BC (2004) Quenching and partitioning response of a Si-added TRIP sheet steel. In: International Conference on Advanced High Strength Sheet Steels for Automotive Applications Proceedings. Warrendale
3. World Steel Association AISBL (2021) A new global formability diagram. https://ahssinsights.org/blog/a-new-global-formability-diagram/. Accessed 4 Apr 2024
4. China Baowu Steel Group Corperation Limited (2012) Q&P (Quenched and Partitioning) Steels. http://rd.baosteel.com/zypt//en/ability/see/abilityDetailsBSSF5/1/318362afb3924a479c3bb4407ce48f6a. Accessed 16 May 2024
5. Clarke AJ, Speer JG, Miller MK et al (2008) Carbon partitioning to austenite from martensite or bainite during the quench and partition (Q&P) process: a critical assessment. Acta Materialia 56:16–22. https://doi.org/10.1016/j.actamat.2007.08.051
6. Wang L, Speer JG (2013) Quenching and partitioning steel heat treatment. Metallogr Microstruct Anal 2:268–281. https://doi.org/10.1007/s13632-013-0082-8
7. Janda T, Jirkova H, Jenicek S (2018) Comparing properties of the 42SiCr steel after conventional heat treatment and QP processing. In: Katalinic B (ed) DAAAM Proceedings, 1st ed. DAAAM International Vienna, pp 1164–1167. https://doi.org/10.2507/29th.daaam.proceedings.167
8. De Moor E, Lacroix S, Clarke AJ et al (2008) Effect of retained austenite stabilized via quench and partitioning on the strain hardening of martensitic steels. Metall Mater Trans A 39:2586–2595. https://doi.org/10.1007/s11661-008-9609-z
9. Ariza-Echeverri EA, Masoumi M, Nishikawa AS et al (2020) Development of a new generation of quench and partitioning

steels: influence of processing parameters on texture, nanoindentation, and mechanical properties. Mater Des 186:1–17. https://doi.org/10.1016/j.matdes.2019.108329
10. Jirková H, Mašek B, Wagner MF-X et al (2014) Influence of metastable retained austenite on macro and micromechanical properties of steel processed by the Q&P process. J Alloys Compd 615:163–168. https://doi.org/10.1016/j.jallcom.2013.12.028
11. Thyssenkrupp Steel Europe AG (2022) New product development in collaboration with JFE Steel Corporation. https://www.thyssenkrupp-steel.com/media/content_1/presse/dokumente/2022/april_6/20220404_tkse_jfe_eng.pdf. Accessed 31 May 2024
12. Mašek B, Jirková H, Hauserova D et al (2010) The effect of Mn and Si on the properties of advanced high strength steels processed by quenching and partitioning. MSF 654–656:94–97. https://doi.org/10.4028/www.scientific.net/MSF.654-656.94
13. Černý I, Mikulová D, Sís J et al (2011) Fatigue properties of a low alloy 42SiCr steel heat treated by quenching and partitioning process. Procedia Eng 10:3310–3315. https://doi.org/10.1016/j.proeng.2011.04.546
14. Thomä M, Wagner G (2021) Effect of quenching and partitioning heat treatment on the fatigue behavior of 42SiCr steel. Metals 11:1–13. https://doi.org/10.3390/met11111699
15. Bublíková D, Jirková H, Jeníček Š, Káňa J (2018) Q&P process in press-hardening of 42SiCr steel. Acta Metall Slovaca 24:52–57. https://doi.org/10.12776/ams.v24i1.967
16. Zhu B, Zhu J, Wang Y et al (2018) Combined hot stamping and Q&P processing with a hot air partitioning device. J Mater Process Technol 262:392–402. https://doi.org/10.1016/j.jmatprotec.2018.07.011
17. Frohn Sörensen P, Mašek B, Wagner MF-X et al (2020) Flexible manufacturing chain with integrated incremental bending and Q-P heat treatment for on-demand production of AHSS safety parts. J Mater Process Technol 275:1–14. https://doi.org/10.1016/j.jmatprotec.2019.116312
18. Somani MC, Porter DA, Karjalainen LP, Misra RDK (2014) On various aspects of decomposition of austenite in a high-silicon steel during quenching and partitioning. Metall and Mat Trans A 45:1247–1257. https://doi.org/10.1007/s11661-013-2053-8
19. Jeníček Š, Vrtáček J, Vorel I, Janda T (2020) Dilatometric identification of bainitic transformation during Q-P processing of 42SiCr medium carbon steel. Manuf Technol 20:327–334. https://doi.org/10.21062/mft.2020.057
20. Jirková H, Kučerová L, Mašek B (2015) The effect of chromium on microstructure development during Q-P process. Mater Today Proc 2:627–630. https://doi.org/10.1016/j.matpr.2015.07.362
21. Härtel S, Awiszus B, Graf M et al (2019) Influence of austenite grain size on mechanical properties after quench and partitioning treatment of a 42SiCr steel. Metals 9:1–11. https://doi.org/10.3390/met9050577
22. Rubešová K, Vorel I, Jirková H, Jeníček Š (2018) Effects of Q&P process parameters on properties of 42SiCr steel. Acta Metall Slovaca 24:126–133. https://doi.org/10.12776/ams.v24i2.1063
23. Khalaj O, Jamshidi M (Behdad), Hassas P, et al (2022) Metaverse and AI digital twinning of 42SiCr steel alloys. Mathematics 11:1–23.https://doi.org/10.3390/math11010004
24. Tikhe O, Doiphode P, Nichul U et al (2023) Development of optimized mechanical properties of AISI 4340 steel: role of quenching and partitioning process. Met Mater Int 29:1–12. https://doi.org/10.1007/s12540-022-01375-6
25. Wang B, Duan QQ, Yao G et al (2014) Investigation on fatigue fracture behaviors of spot welded Q&P980 steel. Int J Fatigue 66:20–28. https://doi.org/10.1016/j.ijfatigue.2014.03.004
26. Russo Spena P, De Maddis M, D'Antonio G, Lombardi F (2016) Weldability and monitoring of resistance spot welding of Q&P and TRIP steels. Metals 6:1–15. https://doi.org/10.3390/met6110270
27 Peković M, Jeníček Š, Rubešová K et al (2018) Welding of 42SiCr high-strength steel. Manuf Technol 1:84–89. https://doi.org/10.21062/ujep/58.2018/a/1213-2489/MT/18/1/84
28. Nadimi N, Yadegari R, Pouranvari M (2023) Resistance spot welding of quenching and partitioning (Q&P) third-generation advanced high-strength steel: process–microstructure–performance. Metall Mater Trans A 54:577–589. https://doi.org/10.1007/s11661-022-06903-y
29. Liu XD, Xu YB, Misra RDK et al (2019) Mechanical properties in double pulse resistance spot welding of Q&P 980 steel. J Mater Process Technol 263:186–197. https://doi.org/10.1016/j.jmatprotec.2018.08.018
30. Zhang Y, Xu W, Zhang G et al (2022) Mechanical behavior and failure mechanism of Q&P980 steel during in situ post-weld heat treatment (PWHT) resistance spot welding. Metall Mater Trans A 53:794–809. https://doi.org/10.1007/s11661-021-06546-5
31. Figueredo B, Ramachandran DC, Macwan A, Biro E (2021) Failure behavior and mechanical properties in the resistance spot welding of quenched and partitioned (Q&P) steels. Weld World 65:2359–2369. https://doi.org/10.1007/s40194-021-01179-z
32. Kroll M, Birnbaum P, Zeisig J et al (2019) Manufacturing of 42SiCr-pipes for quenching and partitioning by longitudinal HFI-welding. Metals 9:1–15. https://doi.org/10.3390/met9060716
33. Dittrich F, Kaars J, Masek B et al (2019) HAZ characterization of welded 42SiCr steel treated by quenching and partitioning. J Mater Process Technol 268:37–46. https://doi.org/10.1016/j.jmatprotec.2018.12.035
34. Xue J, Peng P, Guo W et al (2021) HAZ characterization and mechanical properties of QP980-DP980 laser welded joints. Chin J Mech Eng 34:1–14. https://doi.org/10.1186/s10033-021-00596-x
35. Mehner T, Morgenstern R, Frint P et al (2018) Corrosion characteristics of a quenching and partitioning steel determined by electrochemical impedance spectroscopy. IOP Conf Ser Mater Sci Eng 373:1–8. https://doi.org/10.1088/1757-899X/373/1/012003
36. Çoban O, Kaymak F, Gürol U, Koçak M (2025) Characterization of fillet welded armor steel performed by robotic gas metal arc welding: effect of heat input on microstructure and microhardness. J Materi Eng Perform 34:231–244. https://doi.org/10.1007/s11665-023-09058-y
37. Gürol U, Karahan T, Erdöl S et al (2022) Characterization of armour steel welds using austenitic and ferritic filler metals. Trans Indian Inst Met 75:757–770. https://doi.org/10.1007/s12666-021-02464-7
38. Jia Q, Guo W, Wan Z et al (2018) Microstructure and mechanical properties of laser welded dissimilar joints between QP and boron alloyed martensitic steels. J Mater Process Technol 259:58–67. https://doi.org/10.1016/j.jmatprotec.2018.04.020
39. Vorel I, Opatova K, Rubesova K, et al (2015) Analysis of laser welds on steel processed by Q P process. In: Fourth international conference on advances in mechanical, aeronautical and production techniques - MAPT 2015. Institute of Research Engineers and Doctors, pp 29–32